On the origin of the giant magnetocaloric effect in HoMn2O5 single crystals: First principles study and Monte Carlo simulations

Hamza Bouhani, A. Endichi, H. Zaari, A. Benyoussef, M. Hamedoun, M. Balli, A. El Kenz, O. Mounkachi

On the origin of the giant magneto-caloric effect in HoMn_2O_5 single crystals: First principles study and Monte Carlo simulations

H. Bouhani[a,b], A. Endichi[a,b], H. Zaari[a], A. Benyoussef[c,d], M. Hamedoun[c], M. Balli[e], El. Kenz[a], O.Mounkachi[a]

[a] Laboratory of Condensed Matter and Interdisciplinary Sciences (LaMCSci), B.P. 1014, Faculty of science, Mohammed V University, Rabat, Morocco

[b] Institut Jean Lamour, UMR CNRS 7198, Université de Lorraine, Boite Postale 70239, F-54506 Vandoeuvre-lès-Nancy, France

[c] MAScIR Foundation, Institute of Nanomaterials and Nanotechnologies, Materials & Nanomaterials Center, B.P. 10100 Rabat, Morocco

[d] Hassan II Academy of Science and Technology, Rabat, Morocco

[e] Université de Sherbrooke, Département de physique, J1K 2R1 Quebec, Canada

Abstract

Large rotating magneto-caloric effect (MCE) has been recently observed in $HoMn_2O_5$ single crystal due to the strong magneto-crystalline anisotropy making a significant step towards efficient magnetic refrigeration systems. We tried to explain, theoretically, the reasons behind the magnificent performance in terms of magneto-caloric effect based on DFT calculations and Monte Carlo simulations. X-ray magnetic circular dichroism (XMCD) was performed in order to disentangle the magnetic contribution responsible for the MCE, as well as, the investigation of electronic and magnetic properties. The obtained results would enable the understanding of electronic and magnetic behaviors experimentally observed in $HoMn_2O_5$ single crystal and also the optimization the MCE for magnetic refrigeration.

KEYWORDS: Magneto-caloric effect, anisotropy, XMCD, magnetism, First principles calculations.

I. Introduction

Multiferroic materials have been intensively studied over the past decade for their high interest and their potential applications in the field of spintronic [1]. Indeed, these multifunctional systems are usually characterized by a fundamental state involving a strong interplay between magnetism and ferroelectricity [2-3], opening the way for several future applications.

One of the fields of great interest is the magneto-caloric effect. Recently, a large rotating MCE was experimentally observed in multiferroics RMn_2O_5 (R=Ho,Tb) [4-6]. Following this discovery, an innovative concept for the liquefaction of helium and hydrogen using the rotating MCE was proposed [3] which is an important step towards the development of magnetic refrigeration. It is worth noting that the majority of existing prototypes and patents are based on the rotation of magneto-caloric materials in a magnetic field since there is a much lower contribution of the magneto-crystalline anisotropy to the magnetoc-caloric effect at the magnetic phrase transition when compared to that generated by the change of magnetic transition [7].

These multiferroics materials are usually frustrated magnets whose spin-spin and spin-lattice interactions exclude the simple magnetic arrangement of spins. The consequences of their frustrated magnetic structures are spectacular, it manifests mainly as the strong correlation between magnetic and electrical properties [8].

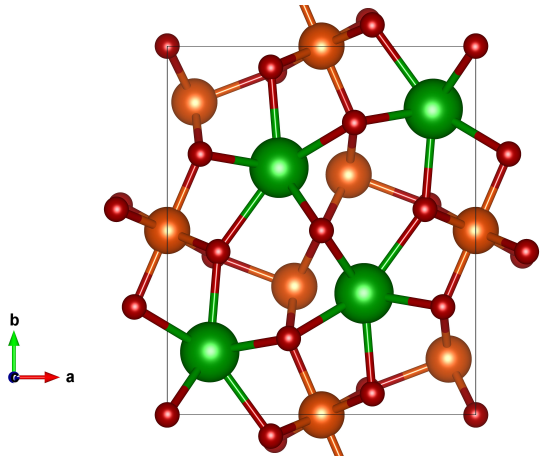

(a)

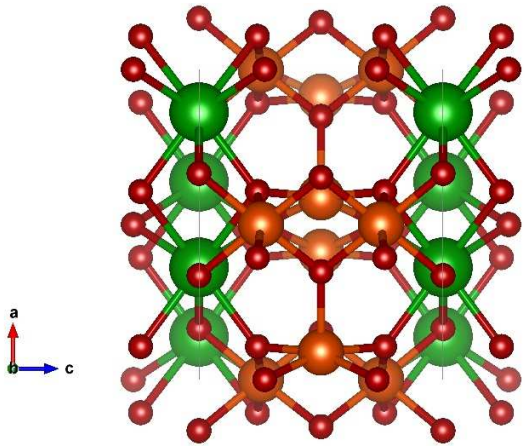

(b)

FIG. 1. (a) Side view and (b) top view along b axis of the crystallographic structure of $HoMn_2O_5$ single crystals. The green spheres are holmium atoms, the orange stands for the manganese atoms and the red corresponds to oxygen atoms.

The RMn_2O_5 compounds (R = rare earth) have an orthorhombic structure [9] consisting of $Mn^{4+}O_6$ octahedral and $Mn^{3+}O_5$ bipyramids connected by their edges and corners. This structure is illustrated in FIG.1. Perfect knowledge of magnetic orders involving Mn^{3+} and Mn^{4+} ions is essential for a better understanding of multiferroic features in RMn_2O_5 compounds. Recent studies of RMn_2O_5 compounds show rich magnetic properties [3-4]. The majority of these materials present at least four magnetic transitions: a first transition occurs at $T_1 = 42 – 45$ K in which the spins of Mn ions adopt a sinusoidal incommensurate (ICM) order. Then, another transition takes place at $T_2 = 38\text{-}41$ K where the spins are configured in a commensurate (CM) antiferromagnetic order then a return to sinusoidal incommensurate order at $T_3 = 18$ K. Below 10 K, the magnetic order of the rare earth ions appears and adopts an incommensurate antiferromagnetic order, becoming commensurate on further cooling [9]. A dielectric constant step is observed at the CM-ICM magnetic phase transition [10] being the key to understand the strong magnetoelectric correlation which is indicated by the modification of dielectric function due to the ordering of Mn spins [11]. In this work, we mainly focus on the electronic, magnetic and magnetocaloric properties of $HoMn_2O_5$ single crystal and therefore, explain the reasons behind the large rotating magneto caloric effect recently observed in $HoMn_2O_5$ crystals [3].

II. Computational details

All calculations were done using the Full Potential Augmented Plane Wave (FP-LAPW) method implemented in WIEN2K code[12] based on density functional theory [13] with the exchange correlation functional treated in the Generalized Gradient Approximations [14] taking into account the spin orbit interactions. To investigate the magnetic properties, we have used 7*6*9 Monkhorst-Pack scheme [15], the total energy was converged to less than 10^{-6} Ryd and the cut-off energy is set to -8.0 Ryd. The radii of the muffin-tin spheres were: R_{MT} (Ho) = 2.53, R_{MT} (Mn1) = 1.86, R_{MT} (Mn2) = 1.97 and R_{MT} (O) = 1.67 a.u (atomic units). Moreover, magnetic anisotropy is calculated using DIPAN program [16, 25] that calculate the dipolar magneto-crystalline anisotropy and the magnetic dipolar hyperfine field by a direct lattice summation over the magnetic moment of all the sites.

In order to disentangle the magnetic contribution responsible for the magneto-caloric effect in $HoMn_2O_5$, we have studied the differentiated role of Ho and Mn ions using XMCD and XAS spectrum. Therefore, we calculated, separately, the values of both spin and orbital magnetic moment.

XMCD represents the absorption difference between the right circular polarization (μ^+) and the left circular polarization (μ^-). The left and right directions are referenced to the propagation direction of the incident radiation while respecting the axis of the magnetic field. In particular, the photons are polarized left (right). When the direction of propagation is antiparallel, their helicity is - ħ (+-ħ) [17].

The objective of XMCD spectrum is to determine the orbital and spin moment, knowing that there is a relationship between the integral of the XMCD spectrum and the mean value of the projection of the orbital angular momentum on the magnetization axis. This relationship was suggested by TholeCarra and Van Der Laan [18], later, the same authors proposed a second sum rules for spin moment [19]

$$\frac{\int_{j^+} d\omega\left(\mu^+ - \mu^-\right)}{\int_{j^\pm} d\omega\left(\mu^+ + \mu^- + \mu^0\right)} = \frac{1c(c+1) - l(l+1) - 2}{2l(l+1)(4l+2-n)} . < Lz > \tag{I.1}$$

$$\frac{\int_{j^+} d\omega\left(\mu^+ - \mu^-\right) - c(c+1)\int_{j^-} d\omega\left(\mu^+ - \mu^-\right)}{\int_{j^\pm} d\omega\left(\mu^+ + \mu^- + \mu^0\right)} = \frac{l(l+1) - c(c+1) - 2}{3c(4l+2-n)} < Sz > \tag{I.2}$$

- l = orbital quantum number of the valence state

- c = orbital quantum number of the core state

- (μ^+) (μ^-) = absorption spectrum for left (right) circularly polarized light.

- <Tz>= expectation value of magnetic dipole operator

The sum rules allow to obtain separately the orbital magnetic moment <Lz> and the spin magnetic moment <Sz> [17] from the integrated XMCD.

For $M_{4,5}$ the transition from 3*d* (l=2) to 4*f* (l=3):

$$ms = (\mu_b / \hbar)\langle Sz \rangle =$$
$$((7\int_{M5} d\omega(\mu^+ - \mu^-) - 6\int_{M4} d\omega(\mu^+ - \mu^-)) / (\int_{M4+M5} d\omega(\mu^+ + \mu^-)) * \left(14 - n_{4f}\right)\left(1 + 10(\langle Tz \rangle / \langle Sz \rangle)\right)^{-1}$$
$$m_L = (\mu_b / \hbar)\langle Lz \rangle = -2((\int_{M_4+M5} d\omega(\mu^+ - \mu^-)) / \int_{M4+M5} d\omega(\mu^+ + \mu^-)) * \left(14 - n_{4f}\right) \tag{I.3}$$

For L_{23}, the transition from 2*p* (l=1) to 3*d* (l=2):

$$m_L = \frac{\mu_b}{\hbar}\langle Lz \rangle = -\frac{4}{3}\frac{\int_{L_3+L_2} d\,\omega(\mu^+ - \mu^-)}{\int_{L_3+L_2} d\,\omega(\mu^+ + \mu^-)}(10 - n_{3d}) \quad \text{(I.4)}$$

$$ms = \frac{\mu_b}{\hbar}\langle Sz \rangle = -\frac{6\int_{L_3} d\,\omega(\mu^+ - \mu^-) - 4\int_{L_3+L_2} d\,\omega(\mu^+ - \mu^-)}{\int_{L_3+L_2} d\,\omega(\mu^+ + \mu^-)}(10 - n_{3d})\left(1 + \frac{7}{2}\frac{\langle Tz \rangle}{\langle Sz \rangle}\right)^{-1} \quad \text{(I.5)}$$

A strong magneto-crystalline anisotropy is experimentally observed in $HoMn_2O_5$ single crystals where the magnetization tends to orient preferentially along the b-axis [3, 20]. In order to get more insight on the gigantic anisotropy shown by this compound, the energy of the system following each axis has been calculated using DIPAN program implemented in WIEN2k package.

III. Results and Discussions :

1. Electronic properties

We have displayed the density of state using GGA approximation to describe the magnetic and electronic properties shown in FIG.2. The main contribution to the magnetism comes from 4*f* states of Holmium which is responsible for the magnetic moment formation on Holmium atoms. The oxygen-manganese molecular bond is formed by *p* electrons of oxygen and *s* electrons of manganese. Each oxygen atom is twice ionized, involving two electrons in its *p* orbitals. The ionization of the manganese atom depends on the chemical formula of the compound: Mn is 4 times ionized, Mn^{3+} and Mn^{4+} are deficient in electrons, respectively involving 4 and 3 electrons in its *d* layers. In the absence of perturbation, the manganese *d* orbitals are degenerate but in a crystal field of given symmetry. The crystal matrix favors an arrangement of some orbitals by partially lifting their degeneration. For $HoMn_2O_5$ compound, Mn occupies two sites of different symmetry: Mn^{4+} at the center of an octahedron and Mn^{3+} at the center of a pyramid. Each symmetry acts differently on the distribution of the electronic levels of Mn. The d orbitals are divided into two sub-groups for octahedral and tetragonal

symmetries: at t2g level of low triple-degenerate and another level doubly degenerate Eg. As expected, we can see that the degeneracy of its *d* orbital is lifted especially in Dz^2 lodge. This anomaly is known as the crystal field deformation or Jahn Teller effect [21].

One can also notice that 4*f* Holmium orbitals favors the spin orbit coupling effect while the 3*d* orbitals of manganese favors the crystalline field. T_{2g} levels have dxy, dyz and dxz orbital character lying on the same level while there is separation in energy between the e2g pics which indicate a deformation field or splitting in Mn1. In the contrary, the partial density of states for Mn_2 shows a t2g splitting with a 2/3 filled band while there is no e2g splitting as shown in FIG.3.

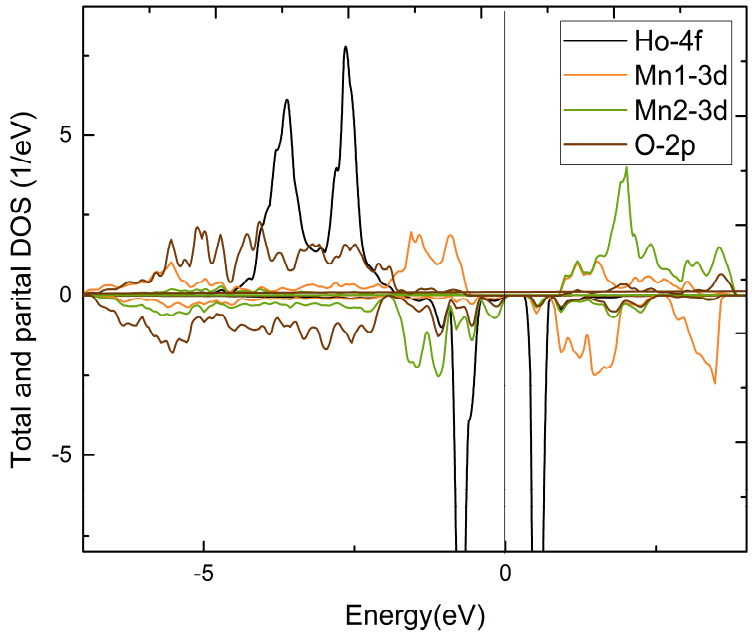

FIG. 2. The total and partial density of states obtained within (GGA+ Spin Orbit)

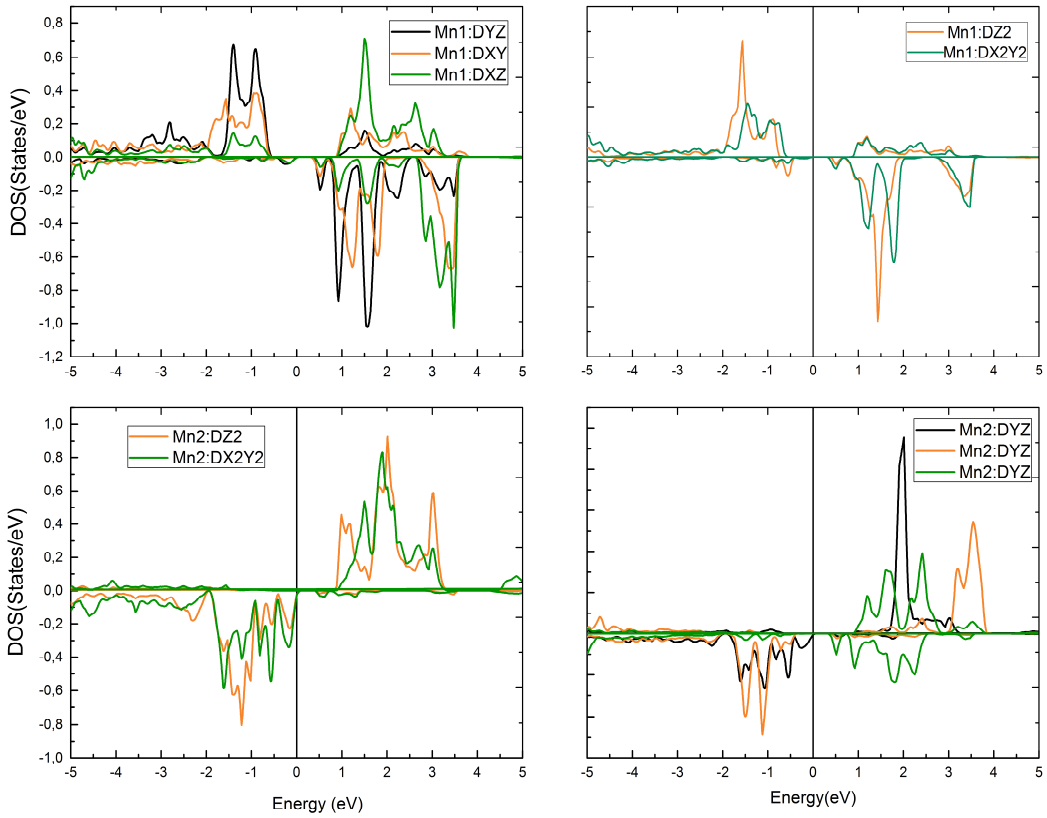

FIG. 3. The partial density of states for Mn_1 (3d) and Mn_2 (3d)

2. Magnetic properties

As mentioned in the introduction, $HoMn_2O_5$ single crystals shows an interesting magnetic properties following a specific direction. Indeed, the calculation of the energy of each axis demonstrate that system has its lowest energy following the b-axis which has been reported in experimental data [3].

The high magnetic moment of Holmium atoms makes the compound an excellent candidate for MCE materials. Therefore, we calculate that spin and orbital magnetic moment, separately, using XMCD spectrum to disentangle the magnetic contribution responsible for the MCE in $HoMn_2O_5$ single crystals.

A. XMCD at the Ho $M_{4,5}$ edge

The absorption edge that provides the most direct information for the rare earth 3d-4f transitions is the $M_{4,5}$ edge. The theoretical treatment of that edge is generally done using a model where the interactions with the environment such as the crystal field are considered to be of weak perturbation except for systems where the rare earth exhibits valence instability or mixed valence [22]. This approach is valid due to localized Ho 4f electrons and there is therefore no overlap between the 4f levels of two neighboring atoms.

In FIG.4, the Ho 3*d*-4*f* absorption spectrum is characterized by M_4 and M_5 that are separated in energy by the strong spin-orbit effect. At M_5 edge, the intensity is very high compared to M_4 edge indicating a large contribution of the orbital moment. We calculated, therefore, the spin and orbital magnetic moment. The values are as follows:

Tab. 1. Spin, orbital and total magnetic moment for Ho, Mn_1 and Mn_2

	XMCD			Experimental
	Ho	Mn_1	Mn_2	Ho
Spin moment (μ_B)	7.77			
Orbital moment (μ_B)	2.44	0.066	-0.14	
Total moment (μ_B)	10.21	2.79	-2.58	10.3 [24]

The expected value of a free Ho^{3+} ($4f^{10}$) magnetic moment with respect to hund's rule ground state (J=8, S=2 and L=6) is 10.3 μ_B taking into consideration that the atom is considered as isolated whereas, it is necessary to take into account the atomic environment.

The negative (positive) signal indicates a parallel alignment of Ho sublattice to the applied magnetic field and may refer to a double transition: 3*d* to 4*f* and 4*f* to 5*s* known as the quadrupole transition. FIG.4 (b) represents the integral of XAS (XMCD) that allow the calculation of the spin and orbital magnetic moment.

B.XMCD at the Mn $L_{2,3}$ edge

We tried now to acquire in depth information about the magnetic contribution from the Mn ions. The results shown in Tab.1, indicates that only a small magnetic moment is induced within the antiferromagnetic cycloidal configuration confirming that along the easy axis b, the contribution of the Mn lattice to the full magnetization is negligible and mainly originates from the Ho^{3+}sublattice.[3].

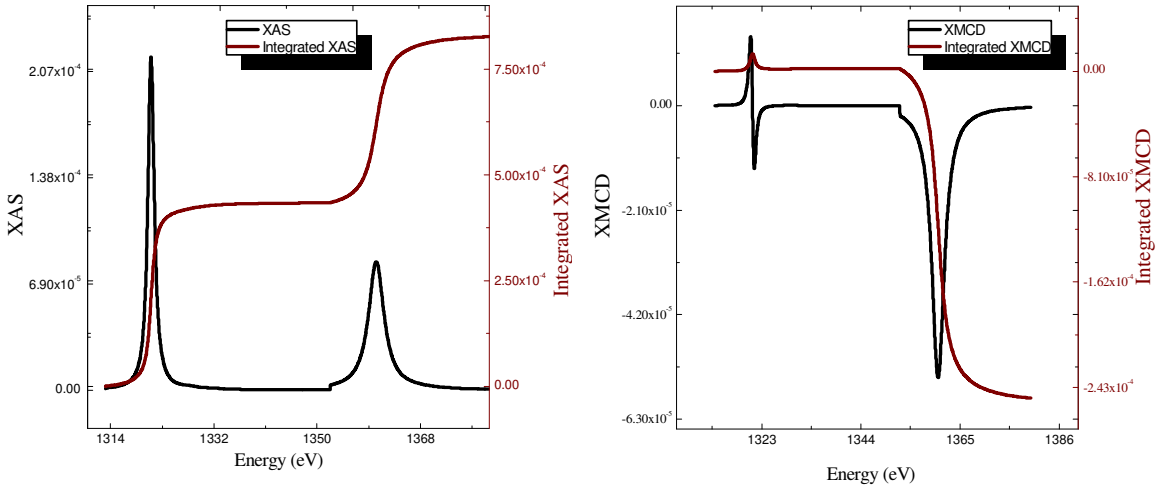

(a) (b)

FIG. 4. (a) XAS spectra representing M4.5 (wine line) and the integral of the spectra (black line) within GGA approximation and (b) XMCD spectra representing M4.5 (wine line) and the integral of the spectra (black line) within GGA approximation

3. Magnetocaloric properties

To investigate the magneto-caloric effect in $HoMn_2O_5$ single crystal, a classical model that combines both Ising and XY models was proposed to deal with the anisotropy since the manganese spin's components can be oriented in any direction in a two-dimensional plane while the holmium's spin components direction are either parallel or antiparallel. Indeed, the spins are represented by two-component vectors that satisfy the $\sigma_i^2 = \sigma_{ix}^2 + \sigma_{iy}^2$ constraint.

The proposed hamiltonian is:

$$H = -J_1 \sum_{<i,j>} \overrightarrow{\sigma_1^1}\,\overrightarrow{\sigma_j^1} - J_2 \sum_{<i,j>} \overrightarrow{\sigma_1^2}\,\overrightarrow{\sigma_j^2} - J_3 \sum_{<i,j>} \overrightarrow{\sigma_1^1}\,\overrightarrow{\sigma_j^2} - J_4 \sum_{<i,j>} \overrightarrow{\sigma_1^1}\,\overrightarrow{\sigma_j^2} - J_5 \sum_{<i,j>} \sigma_{iy}{}^2\, S_{jy} - J_6 \sum_{<i,j>} \sigma_{iy}{}^1\, S_{jy} -$$
$$J_7 \sum_{<i,j>} S_{iy}\, S_{jy} - J_8 \sum_{<i,j>} S_{iy}\, S_{jy} - h \sum_i \overrightarrow{\sigma_1^1} - h \sum_i \overrightarrow{\sigma_1^2} - \sum_{<i,j>} S_{iy} \qquad \text{(I.7)}$$

Where:

S_{iy}: Holmium spin, σ_1: $Manganese\ Mn^{4+}\ spin$ and σ_2: $Manganese\ Mn^{3+}$ spin

J_1: Interaction coupling between first Mn^{4+} nearest neighbors

J_2: Interaction coupling between first Mn^{3+} nearest neighbors

J_3: Interaction coupling between first $Mn^{4+} - Mn^{3+}$ nearest neighbors

J_4: Interaction coupling between second $Mn^{4+} - Mn^{3+}$ nearest neighbors

J_5: Interaction coupling between first $Ho^{3+} - Mn^{3+}$ nearest neighbors

J_6: Interaction coupling between first $Ho^{3+} - Mn^{4+}$ nearest neighbors

J_7: Interaction coupling between first Ho^{3+} nearest neighbors

J_8: Interaction coupling between second Ho^{3+} nearest neighbors

With

$\overrightarrow{\sigma_i^1} = \begin{pmatrix} \sigma_{ix}^1 \\ \sigma_{iy}^1 \end{pmatrix}$, $\overrightarrow{\sigma_i^2} = \begin{pmatrix} \sigma_{ix}^2 \\ \sigma_{iy}^2 \end{pmatrix}$ and h: External magnetic field.

The MCE in $HoMn_2O_5$ single crystal is studied based on Monte Carlo simulation using the hamiltonian given by Eq. (I.7) where random spins were chosen and then flipped with Boltzmann based probability using Metropolis algorithm [23] $P_{Met} = \exp.(-\frac{\Delta E}{K_B T})$. The equilibrium properties are reached when averaging the generated configuration starting from different initial conditions. The data generated with 10^6 steps per spin discarding the first 10^4 generated configurations, our calculations were performed for a system with N= 60.

The program used for calculations predicts the following thermodynamic quantities: the magnetization, specific heat and the susceptibility which are given respectively by:

$$M_S = \frac{1}{N} \sum_{i=1}^{N} S_{iy} \text{ and } M_{xy} = \frac{1}{N} . \sqrt{M_x^2 + M_y^2} \qquad \text{(I.7)}$$

$$\chi = \frac{N}{K_b T} [< M_{total}^2 > - < M_{total} >^2] \qquad \text{(I.8)}$$

$$Cv = \frac{1}{K_b T^2} [< E^2 > - < E >^2] \qquad \text{(I.9)}$$

Where E is the internal energy of the system, K_b is the Boltzmann constant and N is the number of spin in each sublattice. The isothermal magnetic entropy change was calculated using an integral version of Maxwell's relation:

$$\Delta S_M\ (T, \Delta H) = -\int_0^{H1} \left(\frac{\partial M(T,H)}{\partial T}\right)_H dH \qquad \text{(I.10)}$$

Where *S, M, H* and *T* are the magnetic entropy, magnetization, applied magnetic field, and the temperature, respectively.

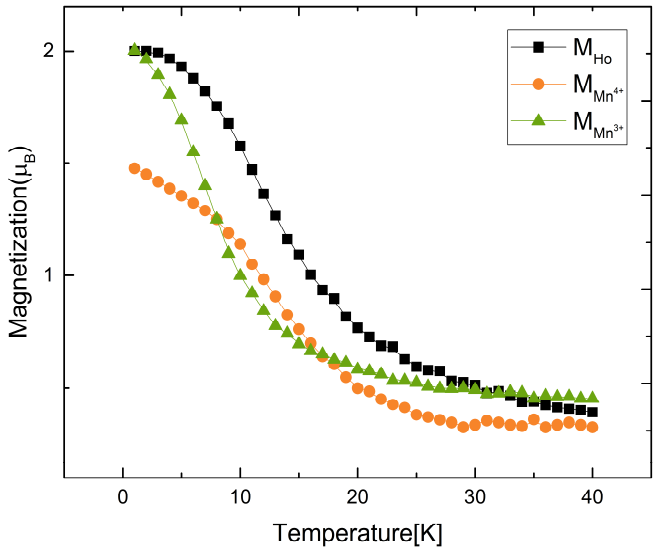

(a)

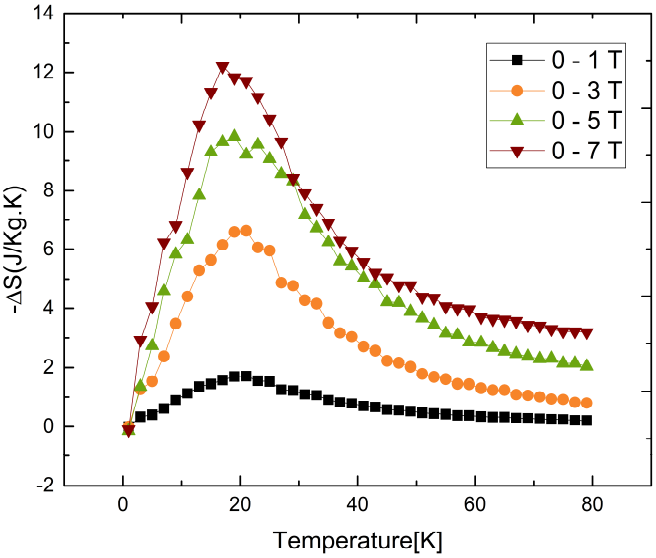

(b)

FIG. 5. (a) Temperature dependence of magnetization following y axis for $HoMn_2O_5$ elements (b) Isothermal magnetic entropy change for different applied magnetic field

Fig.5. (a) presents the temperature dependence of magnetization following b axis for Ho^{3+}, Mn^{3} and Mn^{4+}. |ΔS| values are shown in Fig.5 (b) for several magnetic field. The magnetic field variation from 0 to 7 T yields to a maximum of entropy change of 12.20 J/Kg.K close to the value reported by Balli et al [3] which is about 13.1 J/Kg.K. The maximum of |ΔS| increases with increasing the external magnetic field since the magnetic moments are governed by the interactions of exchange between ions in a magnetic structure passing to a disordered magnetic configuration (paramagnetic region).

Another important parameter that is usually used to compare the MCE is the relative cooling power (RCP) which is defined as the product of the maximum isothermal magnetic entropy and the full width at half maximum and it is given in Fig.6 as the RCP reaches 353 J/Kg for an applied magnetic field of 7 T. These results are comparable with those reported in literature [3]

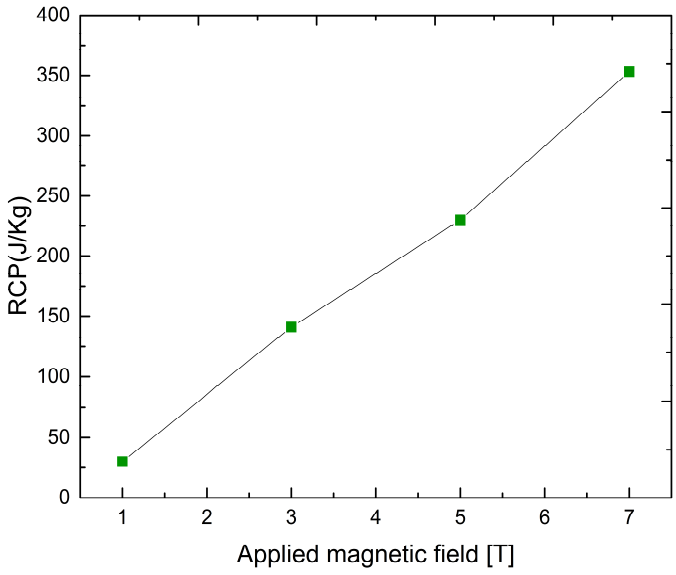

FIG. 6. Relative cooling power (RCP) as a function of the applied magnetic field

Conclusion

First principles calculations reveal that the saturation magnetization reaches it maximum following the easy axis b. The same calculations shows that the main contribution to the MCE comes from Ho ions. The MCE effect in $HoMn_2O_5$ single crystal is studied based on Monte Carlo simulations giving similar results compared to experimental study. This work confirms that the use of the intrinsic anisotropic properties is a promising way to optimize the MCE for magnetic refrigeration application at low temperature regime.

Compliance with ethical standards

Conflit of interest The authors declare there is no conflict of interest.

Acknowledgments

This work was supported by the PHC Toubkal/17/49 project.

Reference

[1] S.-W. Cheong, M. Mostovoy, Multiferroics: a magnetic twist for ferroelectricity, Nat. Mater. 6 (2007) 13. https://doi.org/10.1038/nmat1804.

[2] K. Aizu, Possible Species of Ferromagnetic, Ferroelectric, and Ferroelastic Crystals, Phys. Rev. B. 2 (1970) 754–772. doi:10.1103/PhysRevB.2.754.

[3] M. Balli, S. Jandl, P. Fournier, M.M. Gospodinov, Anisotropy-enhanced giant reversible rotating magnetocaloric effect in HoMn2O5 single crystals, Appl. Phys. Lett. 104 (2014) 232402. doi:10.1063/1.4880818.

[4] M. Balli, S. Jandl, P. Fournier, D.Z. Dimitrov, Giant rotating magnetocaloric effect at low magnetic fields in multiferroic TbMn2O5 single crystals, Appl. Phys. Lett. 108 (2016) 102401. doi:10.1063/1.4943109.

[5] Y. Noda, H. Kimura, M. Fukunaga, S. Kobayashi, I. Kagomiya, K. Kohn, Magnetic and ferroelectric properties of multiferroic RMn2O5, J. Phys. Condens. Matter. 20 (2008) 434206. doi:10.1088/0953-8984/20/43/434206.

[6] P. Fournier, Giant rotating magnetocaloric effect at low magnetic fields in multiferroic TbMn2O5 single crystals, Crystals 7 44 (2016). doi:10.1063/1.4943109.

[7] S.A. Nikitin, K.P. Skokov, Y.S. Koshkid'ko, Y.G. Pastushenkov, T.I. Ivanova, Giant Rotating Magnetocaloric Effect in the Region of Spin-Reorientation Transition in the NdCo5 Single Crystal, Phys. Rev. Lett. 105 (2010) 137205. doi:10.1103/PhysRevLett.105.137205.

[8] N. Hur, S. Park, P. A. Sharma, J. S. Ahn, S. Guha, S-W Cheong,) Electric polarization reversal and memory in a multiferroic material induced by magnetic fields. Nature. (2004); 429(6990): 392–395. doi: 10.1038/nature02572

[9] G.R. Blake, L.C. Chapon, P.G. Radaelli, S. Park, N. Hur, S.-W. Cheong, J. Rodríguez-Carvajal, Spin structure and magnetic

frustration in multiferroic RMn2O5 (R=\ Tb,Ho,Dy), Phys. Rev. B. 71 (2005) 214402. doi:10.1103/PhysRevB.71.214402.

[10] K. Cao, G.-C. Guo, D. Vanderbilt, L. He, First-Principles Modeling of Multiferroic RMn2O5, Phys. Rev. Lett. 103 (2009) 257201. doi:10.1103/PhysRevLett.103.257201.

[11] I. Radulov, V.I. Nizhankovskii, V. Lovchinov, D. Dimitrov, A. Apostolov, Colossal magnetostriction effect in HoMn2O5, Eur. Phys. J. B. 52 (2006) 361–364. https://doi.org/10.1140/epjb/e2006-00318-3.

[12] P. Blaha, P. Blaha, K. Schwarz, G.K.H. Madsen, D. Kvasnicka, J. Luitz, (2007) WIEN2k_7.3, An Augmented Plane Wave + Local Orbitals Program for Calculating Crystal Properties, Karlheinz Schwarz, Techn. Uni- versität Wien, Austria

[13] P. Hohenberg, W. Kohn, Inhomogeneous Electron Gas, Phys. Rev. 136 (1964) B864–B871. doi:10.1103/PhysRev.136.B864.

[14] J.P. Perdew, K. Burke, M. Ernzerhof, Generalized Gradient Approximation Made Simple, Phys. Rev. Lett. 77 (1996) 3865–3868. doi:10.1103/PhysRevLett.77.3865.

[15] H.J. Monkhorst, J.D. Pack, Special points for Brillouin-zone integrations, Phys. Rev. B. 13 (1976) 5188–5192. doi:10.1103/PhysRevB.13.5188.

[16] P. Novak´ Inst. of Physics, Acad.Science, Prague, Czeck Republic

[17] B.T. Thole, P. Carra, F. Sette, G. van der Laan, X-ray circular dichroism as a probe of orbital magnetization, Phys. Rev. Lett. 68 (1992) 1943–1946. doi:10.1103/PhysRevLett.68.1943.

[18] P. Carra, B.T. Thole, M. Altarelli, X. Wang, X-ray circular dichroism and local magnetic fields, Phys. Rev. Lett. 70 (1993) 694–697. doi:10.1103/PhysRevLett.70.694.

[19] R. Wu, A.J. Freeman, Limitation of the Magnetic-Circular-Dichroism Spin Sum Rule for Transition Metals and Importance of the Magnetic Dipole Term, Phys. Rev. Lett. 73 (1994) 1994–1997. doi:10.1103/PhysRevLett.73.1994.

[20] M. Balli, P. Fournier, S. Jandl, S. Mansouri, A. Mukhin, Y. V Ivanov, A.M. Balbashov, Comment on ``Giant anisotropy of magnetocaloric effect in TbMnO3 single crystals'', Phys. Rev. B. 96 (2017) 146401. doi:10.1103/PhysRevB.96.146401.

[21] T.-R. Chang, H.-T. Jeng, C.-Y. Ren, C.-S. Hsue, Charge-orbital ordering and ferroelectric polarization in multiferroic TbMn${}_{2}$O${}_{5}$ from first principles, Phys. Rev. B. 84 (2011) 24421. doi:10.1103/PhysRevB.84.024421.

[22] I.M. Band,K.A. Kikoin, M.B. Trzhaskovskaya, and D.I. Khomskii Atomic mechanisms for the appearance of mixed valence states in lanthanides and actinides Zh. Eksp. Teor. Fiz. 94, 79-95 (1988)

[23] N. Metropolis, A.W. Rosenbluth, M.N. Rosenbluth, A.H. Teller, E. Teller, Equation of State Calculations by Fast Computing Machines, J. Chem. Phys. 21 (1953) 1087–1092. doi:10.1063/1.1699114.

[24] Jens Jensen and Allan R. Mackintosh (1991) Rare Earth Magnetism

[25] Peter Blaha, Karlheinz Schwarz, Georg K. H. Madsen, Dieter Kvasnicka, Joachim Luitz, Robert Laskowski, Fabien Tran, Laurence D. Marks: WIEN2k An Augmented Plane Wave + Local Orbitals Program for Calculating Crystal Properties revised edition WIEN2k 18.2 (Release 07/17/2018)